JAAS

PAPER

View Article Online
View Journal | View Issue

Cite this: *J. Anal. At. Spectrom.*, 2025, **40**, 3172

Innovations in battery material quality control: microwave-sustained inductively coupled atmospheric-pressure plasma optical emission spectroscopy (MICAP OES) for elemental analysis

Jorge Pérez-Vázquez, Raquel Serrano, * Guillermo Grindlay, Luis Gras and Juan Mora

The analysis of both major elements (Co, Li, Mn, Ni) and impurities (*e.g.*, Ca, Cd, Cr, Cu, Fe, Na, Pb) in final cathodes and especially in raw materials, is essential for quality control in the Li-based batteries industry. In recent years, microwave-sustained inductively coupled atmospheric-pressure plasma optical emission spectroscopy (MICAP OES) has emerged as a robust analytical technique for trace element determination, even in complex matrices with high concentration of total dissolved solids. Thus, the aim of this study is to evaluate the analytical capabilities of MICAP OES for quality control purposes (major and impurities determination) in the different materials used in the Li-based battery industry (*i.e.*, raw materials, binary and ternary cathodes). The evaluation was conducted in accordance with the only existing regulations, which have been issued by China. Despite the complexity of the samples, no significant spectral interferences were detected for the most sensitive wavelength of the analytes, with the exception of lead (Pb), which showed interference in Mn-containing matrices. Regarding non-spectral interferences, although the method is still susceptible to matrix effects caused by sample concomitants (mainly Li), these can be effectively corrected using matrix-matched calibration standards. Furthermore, with the appropriate selection of operating conditions and the calibration strategies, both major elements and impurities can be determined simultaneously. The detection limits achieved are comparable to those afforded by ICP OES, and allow the analysis of impurities according to the Chinese standard protocols. Finally, the proposed methodology was satisfactorily validated through the analysis of a cathode reference material (NMC 111 BAM S014), 6 commercial raw materials and 9 cathode samples with different composition.

Received 5th May 2025
Accepted 14th August 2025

DOI: 10.1039/d5ja00183h

rsc.li/jaas

Department of Analytical Chemistry, Nutrition and Food Sciences, University of Alicante, PO Box 99, 03080 Alicante, Spain. E-mail: Raquel.serrano@ua.es

Raquel Serrano

My research journey began in the Department of Analytical Chemistry, Nutrition and Food Science at the University of Alicante during my master's studies, where I discovered a complex but fascinating reality: behind every spectroscopic signal lies a system of influences—a MATRIX—that deserves to be understood. So, after that, I decided to take the red pill and pursued a PhD to fully dive into the mysterious world of matrix effects. Since then, I have dedicated my research career to decoding these hidden mysteries through plasma spectroscopy and developing methods to analyse trace elements in various types of samples. After obtaining my PhD with honours, I joined IELAB S.L., where I worked on developing reference materials—an "analytical oracle" to ensure the quality and traceability of results. I then moved to the other side of the system: the world of knowledge transfer, patents, and contracts, working at the University of Alicante's Research Results Transfer Service. After some time as an Industrial Doctorates Agent, I now work at the university's International Projects Office, where I support the management and promotion of international R&D proposals, helping researchers make their ideas cross borders and become real projects. At the same time, I teach as Associate Professor in the Department of Analytical Chemistry, Nutrition and Food Science and actively collaborate with the Analytical Atomic Spectrometry group—where it all began—closing a circle that, much like in the MATRIX, constantly reprograms itself.

1. Introduction

In recent years, the demand for high-capacity electrochemical power sources with long lifetimes has grown. This is due to the rapid increase in the use of electronic mobile devices (*e.g.* smartphones, tablets, laptops, *etc.*), and the development of new pure and hybrid electric vehicles.[1] The ongoing advancement of lithium-ion batteries (LiBs), coupled with the substantial research conducted on their constituent materials, has firmly established this particular battery type as a front-runner within the energy sector.[2] Amongst all variants of LiBs (*e.g.*, lithium cobalt batteries, lithium–iron phosphate batteries, *etc.*), those containing a ternary cathode (NMC) ($LiNi_xMn_yCo_{(1-x-y)}O_2$) have become one of the most commonly used in recent times due to their high capacity, good cycle stability (battery life) and moderate cost.[3] The stoichiometry in which the main elements (*i.e.*, Co, Fe, Li, Mn, Ni, *etc.*) are found in the different cathode materials can significantly affect the performance and cost of the LiBs. Additionally, the presence of some impurities (*i.e.*, Al, Ca, Cd, Cr, Cu, Fe, Mg, Na, Pb, Zn) in the cathode materials plays an important role in the production of them. Consequently, the accurate determination and precise quantification of the primary elements (*i.e.*, Co, Fe, Li, Mn, Ni), in conjunction with the meticulous control of trace impurities in both the starting materials (*e.g.*, $CoSO_4 \cdot 7H_2O$, $FePO_4 \cdot 2H_2O$, Li_2CO_3, $LiOH \cdot H_2O$, $MnSO_4 \cdot H_2O$, $NiSO_4 \cdot 6H_2O$), intermediates and the finished products, becomes particularly important.[4] Indeed, China, as the main global LiBs manufacturers, has developed the only regulatory standards protocols available to date to ensure the quality control of the raw materials employed for cathode production (YS/T 582-2023 (Li_2CO_3),[5] GB/T 26008-2020 (LiOH),[6] HG/T 5918-2021 ($CoSO_4 \cdot 7H_2O$),[7] HG/T 4823-2015 ($MnSO_4 \cdot H_2O$),[8] HG/T 5919-2021 ($NiSO_4 \cdot 6H_2O$),[9] HG/T 4701-2021 ($FePO_4 \cdot 2H_2O$) [10]), and to regulate the stoichiometry of the main elements and the impurities in the final cathode materials (YS/T 798-2012 (NMC),[11] GB/T 20252-2014 (LCO),[12] YS/T 1027-2015 (LFP),[13] GB/T 37202-2018 (LNMO),[14] YS/T 677-2016 (LMO),[15] YS/T 1125-2016 (NCA) [16]).

Elemental analysis of LiBs raw materials and cathodes is performed using inductively coupled plasma optical emission spectroscopy (ICP OES) and inductively coupled plasma mass spectrometry (ICP-MS) due to their multi-elemental capabilities, sample throughput and detection limits at trace and ultra-trace levels. Nevertheless, because of the high concentrations of easily ionizable elements, such as Li, and some transition metals (Co, Fe, Mn, and Ni), both spectral and non-spectral interferences might arise hindering the accurate quantification of impurities. For this reason, several strategies have been proposed in the literature to mitigate these interferences for analysing impurities in various LiBs materials (*i.e.*, $LiPF_6$ electrolyte, $LiFePO_4$ (LFP), lithium cobalt oxide (LCO), NMC cathodes, lithium materials (LiOH, Li_2CO_3)) when using ICP OES and ICP-MS, such as: (i) different sample introduction systems (*e.g.*, fully demountable extended matrix tolerance quartz torch, an argon humidifier, among others);[2,17] (ii) different calibration techniques (*i.e.*, standard addition, matrix-matched standard calibration, internal standardization, *etc.*);[18–21] and (iii) reaction cell technology for spectral interferences reduction in the case of ICP-MS.[22]

In recent years, high-power microwave induced plasmas (MIP) have emerged as a viable alternative to elemental analysis, offering analytical performance comparable to ICP OES.[23–25] However, to date, the use of high-power MIP systems in the analysis of LiBs remains almost unexplored. This fact may be attributable to the comparatively lower energetic plasmas (*i.e.*, lower plasma temperatures) compared with ICP OES, which results in more significant matrix effects especially when operating solutions with high content of easily ionization elements.[26–28] There is only one known study where a high-power MIP has been used for the analysis of NiMH battery residues. In this study, Cruz *et al.*[29] reported quantitative values for the multi-element analysis of diluted sulfuric acid leachates of NiMH battery residues by means of MIP OES (*i.e.*, Hammer cavity) employing a multi-energy calibration (MEC) strategy to mitigate matrix effects.

Within the recent progress in MIPs, previous studies have demonstrated that microwave- sustained inductively coupled atmospheric-pressure plasma (MICAP) provides a more stable discharge for spectrometry applications compared to other high-power MIP systems.[30–33] Indeed, MICAP OES has been employed in the analysis of samples with diverse matrices, including saline solutions (*i.e.*, 0.1 mol L^{-1} Na, 0.25 mol L^{-1} Ca, and 0.03 mol L^{-1} K), with positive results, which suggest that it could be a useful technique for the analysis of battery industry-related samples.[34,35] Thus, the aim of the present study is to evaluate the feasibility of MICAP OES for the quality control (*i.e.*, content of major elements and impurities) in raw materials employed for the production of LiBs and in different Li-based cathodes. To this end, spectral and non-spectral interferences were investigated for 36 emission lines of a total of 15 elements, corresponding to the major elements and the impurities regulated by the Chinese standard protocols for LiB materials (Al, B, Ca, Cd, Co, Cr, Cu, Fe, Li, Mg, Mn, Na, Ni, Pb and Zn) in the presence of different synthetic matrix solutions. Based on the results obtained in that study, optimal experimental conditions were selected to maximize detection capabilities and different calibration strategies were evaluated to mitigate matrix effects. Finally, the developed procedure was validated by analysing a cathode CRM (NMC111 BAM S014), 6 different raw materials (*e.g.*, Li_2CO_3, LiOH, $CoSO_4$, $MnSO_4$, $NiSO_4$ and $FePO_4$) and 9 cathodes samples (*e.g.*, lithium cobalt oxide, lithium iron phosphate, lithium manganese oxide, lithium nickel cobalt aluminium oxide, and 5 lithium nickel manganese cobalt oxide cathodes with different stoichiometries).

2. Experimental

2.1 Reagents

All solutions were prepared using deionised water obtained from a Milli-Q purification system (Millipore, Paris, France). Suprapure nitric acid 69% w w^{-1}, and hydrochloric acid 37% w w^{-1} were obtained from Panreac (Barcelona, Spain). High-purity metal nitrates, including cobalt(II) nitrate tetrahydrate (98%),

iron(III) nitrate nonahydrate (99.0%), manganese(II) nitrate tetrahydrate (98.5%), and nickel(II) nitrate hexahydrate (98%), were purchased from Scharlau (Valencia, Spain). Lithium nitrate (99.995%) was supplied by Merck (Darmstadt, Germany). A multi-elemental ICP standard solution (1000 mg L^{-1}) containing Ag, Al, B, Ba, Bi, Ca, Cd, Co, Cr, Cu, Fe, Ga, In, K, Li, Mg, Mn, Na, Ni, Pb, Sr, Tl, and Zn was obtained from Sigma-Aldrich (Steinheim, Germany).

2.2 Samples

To assess the applicability of MICAP OES for the quality control of LiBs related materials, 6 raw materials commonly employed in cathode manufacturing processes were analysed to evaluate potential matrix effects and elemental recovery during sample preparation. All the materials employed were of battery-grade quality and were obtained from different distributors. The analysed materials were: (i) lithium carbonate (99.9%) (Li_2CO_3); (ii) lithium hydroxide monohydrate (99.995%) ($LiOH \cdot H_2O$); (iii) cobalt(II) sulphate heptahydrate (99%) ($CoSO_4 \cdot 7H_2O$); (iv) manganese(II) sulphate monohydrate (98%) ($MnSO_4 \cdot H_2O$); (v) nickel(II) sulphate hexahydrate (98%) ($NiSO_4 \cdot 6H_2O$); and (vi) iron(III) phosphate dihydrate ($FePO_4 \cdot 2H_2O$). The inclusion of these precursors provides a representative overview of the elemental profiles encountered prior to cathode synthesis.

In addition, 9 cathode samples, including a cathode Certified Reference Material (CRM) (*i.e.* NMC111 BAM S014), a cathode Candidate Certified Reference Material (NMC811, $LiNi_{0.8}Mn_{0.1}Co_{0.1}O_2$) and different cathode samples of lithium transition metal oxides, were selected to represent a wide range of compositions and manufacturing sources. The composition of the different cathodes selected was: (i) four binary Li-based cathodes with different chemistries, including lithium iron phosphate (LFP, $LiFePO_4$), lithium manganese oxide (LMO, $LiMn_2O_4$), lithium nickel cobalt aluminium oxide (NCA, $LiNi_{0.8}Co_{0.15}Al_{0.05}O_2$) and lithium cobalt oxide (LCO, $LiCoO_2$); and (ii) four ternary cathodes showing variable stoichiometries of lithium, nickel, manganese and cobalt (NMCs)—NMC111 ($LiNi_{0.33}Mn_{0.33}Co_{0.33}O_2$), NMC442 ($LiNi_{0.4}Mn_{0.4}Co_{0.2}O_2$), NMC532 ($LiNi_{0.5}Mn_{0.3}Co_{0.2}O_2$), and NMC622 ($LiNi_{0.6}Mn_{0.2}Co_{0.2}O_2$). All these samples, with the exception of both CRMs obtained from the Federal Institute for Materials Research and Testing (BAM), were acquired from various distributors.

Table 1 Composition of major elements remaining in both raw and cathode material digests

		Composition after digestion (mg kg^{-1})				
	Material	Li	Co	Mn	Ni	Fe
Raw materials	Li_2CO_3	1900	—	—	—	—
	LiOH	1700	—	—	—	—
	$CoSO_4$	—	2100	—	—	—
	$MnSO_4$	—	—	3220	—	—
	$NiSO_4$	—	—	—	2200	—
	$FePO_4$	—	—	—	—	3000
Cathodes	LFP	250	—	—	—	1800
	LCO	375	3000	—	—	—
	LMO	200	—	2900	—	—
	NCA[a]	350	600	—	2750	—
	NMC111	375	1000	930	1000	—
	NMC442	375	600	1125	1200	—
	NMC532	375	600	850	1500	—
	NMC622	375	600	550	1775	—
	NMC811	375	300	275	2350	—

[a] 75 ppm of aluminium.

2.3 Sample preparation

All samples were digested in triplicate using an UltraWave oven (Milestone s.r.l., Sorisole, Italy) according to the manufacturer's recommendations adapting the conditions defined in the Chinese standard protocols[5–16] (Table S1 in the SI). For raw materials, 0.15 g of sample were digested with 4 mL of HNO_3 69% w w^{-1}, except for $FePO_4$ for which 4 mL of HCl 37% w w^{-1} were used instead (Table S2). As regards to other cathode materials, 0.15 g of each sample were digested with 4 mL of aqua regia (1 mL of HNO_3 69% w w^{-1} 4 mL of HCl 37% w w^{-1}) (Table S3). After the digestion process, samples were transferred to polyethylene bottles and brought to a final weight of 15 g with ultrapure water. Finally, the digested raw materials and cathodes were, respectively, diluted 1 : 100 and 1 : 200 with ultrapure water. Samples were stored at 4 °C until analysis by MICAP OES.

2.4 Matrix and analyte solutions

Multielemental solutions containing 10 mg kg^{-1} of each analyte were formulated in synthetic matrices designed to replicate the elemental composition of both raw materials and cathode sample digests in accordance with Chinese standard protocols (Table 1). These solutions were used to investigate spectral and non-spectral interferences arising from the main constituents (*i.e.*, Co, Fe, Li, Mn and Ni) commonly found in these types of sample (a detailed discussion on interferences is provided in Sections 3.1 and 3.2). For comparison purposes, a 5% w w^{-1} nitric acid solution was employed as a reference matrix.

2.5 MICAP instrumentation

Elemental analyses were carried out using a MICAP OES 1000 device (Radom Corporation, Pewaukee, USA), whose technical specifications have been detailed in prior studies.[30,31,34,35] The sample introduction system employed consisted of a OneNeb® pneumatic nebulizer (Ingeniatrics, Sevilla, Spain) coupled to a cyclonic spray chamber. This sample introduction system combination was selected to minimize the possible matrix effects caused on aerosol generation and transport.[30,31] All the operating conditions and the emission lines employed through this work, with information about the upper electronic level involved in each electron transition ($E_{upper\ level}$), are gathered in Tables S4 and S5, in the SI, respectively.

3. Results and discussion

As was previously mentioned, China is the only country in the world that has established regulations to ensure the quality of LiBs related materials, which specify the maximum impurity

content (*i.e.*, Al, B, Ca, Cd, Co, Cr, Cu, Fe, Mg, Mn, Na, Ni, Pb, Zn) and the concentration of major elements (Co, Fe, Li, Mn, Ni). These standard procedures include a series of recommendations for sample pretreatment for raw materials and the LCO cathode. However, no information is provided for other types of binary and ternary cathodes (LFP, LMO, NCA and NMCs). Therefore, raw materials and LCO were digested according to Chinese standards procedures (adapted conditions in Table S2) whereas the remaining samples were pretreated according to the procedures recommended by the MW oven manufacturer (Table S3). With the aim of assessing both spectral and non-spectral interferences, as well as optimizing MICAP OES operating conditions, different analyte synthetic solutions simulating the compositions indicated in Table 1 were used. For the sake of comparison, a 5% w w^{-1} nitric acid solution was used as reference.

3.1 Spectral interferences

To evaluate potential spectral interferences, the full spectrum (wavelength range between 194 and 625 nm) was registered operating all the matrix solutions gathered in Table 1 and compared with that obtained for the reference solution, 5% w w^{-1} HNO_3 (Fig. S1). Among the matrices tested, the simplest background was obtained for the lithium one since its main emission lines were specifically located in the 550–600 nm wavelength range. Conversely, more complex backgrounds were obtained for the rest of the matrices due to the appearance of the different atomic and ionic emission lines of the major elements (*i.e.*, Co, Fe, Mn, Ni) present in those solutions. However, non-significant spectral interferences were detected for the most sensitive emission lines selected of the impurity elements (*i.e.*, Al, B, Ca, Cd, Co, Cr, Cu, Fe, Mg, Mn, Na, Ni, Pb, Zn) (Table S5) except for Pb I 405.781 nm, which has interference from the Mn I 405.795 nm line in the matrices with the highest Mn levels (*i.e.*, the $MnSO_4$ raw material and the LMO cathode) (Fig. S2). For these latter matrices, the second most sensitive Pb emission line (Pb I 368.346 nm) should be used instead but at the expense of sensitivity (*i.e.*, Pb I 405.781 nm is 2.3-fold more sensitive than Pb I 368.346 nm) which could compromise the Pb determination in samples with more restrictive regulatory limits (*e.g.*, on the order of a few mg kg^{-1}).

3.2 Non-spectral interferences

To date, most studies on non-spectral interferences in MICAP OES have focused on alkali and alkali earth elements (Li, Na, Ca, *etc.*)[27,34] and no information is available about matrix effects by transition metals. In this study, for the first time, the influence of the major elements present in LiBs related materials (*i.e.*, Co, Fe, Mn and Ni) on both the nebuliser gas flow rate (Q_g) and the atomic and ionic emission signals of the spectral lines of the different elements regulated by the Chinese standard protocols, was evaluated individually and in combination, including mixtures containing high concentrations of Li. Given that the MICAP is equipped with a fixed-power magnetron (1000 W), this parameter was kept constant throughout all experiments in this work. Similarly, sample uptake rate was fixed at 0.5 mL min^{-1} since previous studies have shown this value offers a good compromise in terms of sensitivity and precision.[35]

3.2.1 Influence of the nebulizer operating conditions. As previously reported in the literature, the influence of Q_g in high-power (N_2)-cavities depends on the emission line considered and the nature of the matrix employed.[34,35] Thus, the influence of Q_g for a total of 36 emission lines was evaluated over the different matrices selected. Fig. 1 shows the influence of Q_g on the net emission signal obtained for Mg I 285.213 nm (Fig. 1A, C and E) and Mg II 280.270 nm (Fig. 1B, D and F) for the different matrices evaluated (*i.e.*, raw materials, binary and ternary cathodes) and the reference solution. Both emission lines have been selected to show the general behaviour observed. The results obtained for the rest of the emission lines are included in the SI (Fig. S3). As can be observed, the atomic emission for all the matrices shows an increase with Q_g up to 0.9 L min^{-1} (Fig. 1A, C and E). In the case of ionic emission, the signal obtained for raw material matrices (Fig. 1B) exhibited, in general, a plateau at Q_g 0.5 L min^{-1}, with the exception of the Li 1900 mg kg^{-1} matrix, for which the emission signal decreased from this Q_g onwards. For the binary and ternary cathode matrices (Fig. 1D and F), this plateau was reached at Q_g 0.7 L min^{-1}. Similar findings were obtained for the remaining emission lines evaluated (Fig. S3). These results are consistent with those previously reported for MICAP OES operating saline solutions (*i.e.*, 0.1 mol L^{-1} Na, 0.25 mol L^{-1} Ca, and 0.03 mol L^{-1} K) and prove that, unlike other high-power (N_2)-cavities, MICAP OES showed a good tolerance working with matrices containing high total dissolved solids.[34,35] In fact, after running the instrument for several hours (>5 h), no significant salt deposits were noticed within the torch. Based on these findings, Q_g 0.9 L min^{-1} was selected as a common condition for performing simultaneous multielement analysis.

In agreement with previous studies in the literature,[26,36,37] it was observed that the matrix might affect both atomic and ionic emission significantly. For atomic emission lines (Fig. 1A, C and E), no significant changes were registered for any of the matrices evaluated regarding the reference solution, with the exception of the Li 1900 mg kg^{-1} matrix, for which a 1.6-fold increase in the emission signal, approximately, was registered for Mg I 285.280 nm at Q_g 0.9 L min^{-1}. Conversely, for the Mg II 280.270 nm, the emission signal was found to be negatively affected in the presence of the different matrices regarding the reference solution (Fig. 1B, D and F). For instance, when operating raw material-based solutions at Q_g 0.9 L min^{-1}, ionic emission was reduced by approximately 20% for the Co, Fe, Mn and Ni matrices, and 60% for the Li matrix. However, a 30% decrease in the emission signal was observed for cathode-based solutions.

These behaviours are similar to the data previously reported operating saline matrices (0.1 mol L^{-1} Na, 0.25 mol L^{-1} Ca, and 0.03 mol L^{-1} K) in MICAP OES,[34] but contrary to the observations made by Hallwirth *et al.*,[27] who encountered signal decrease for both atomic and ionic emission lines when operating a 50 mg kg^{-1} Li solution. The origin of these discrepancies is not clear, but it might be related to the different experimental setup (*i.e.*, nebulizer, torch injector tube internal diameter and

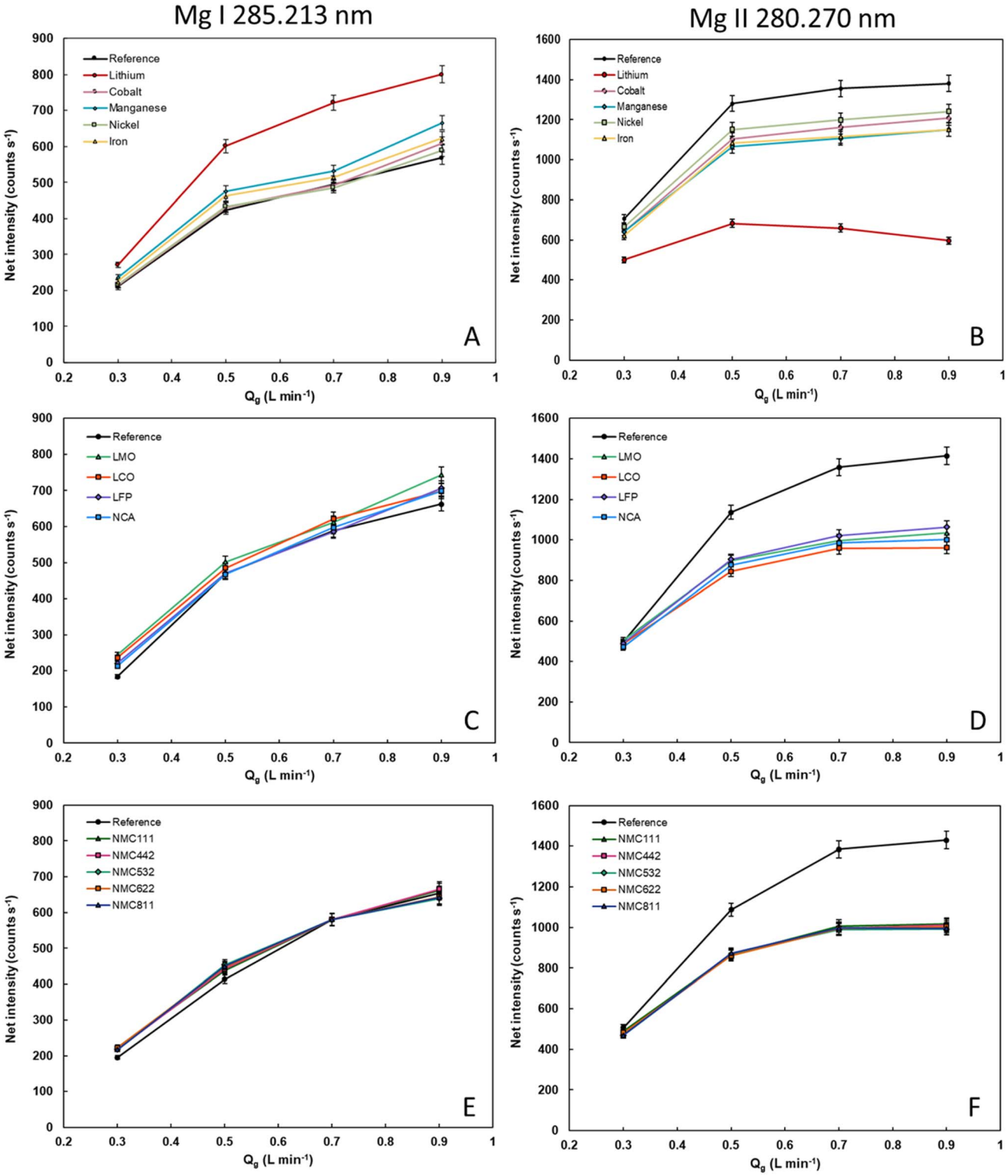

Fig. 1 Influence of the nebulization gas flow rate (Q_g) on the net emission intensity for Mg I 285.213 nm and Mg II 280.270 nm operating the solutions related to raw materials (A and B), binary (C and D) and ternary cathodes (E and F). Q_l 500 μL min^{-1}; TExposure 1000 ms.

spectrometer design) and operating conditions employed in both works.

3.2.2 Influence of the wavelength characteristics. To gain insight into non-spectral interferences by transition metals on both atomic and ionic emission, additional experiments were carried out covering different elements and wavelength characteristics (*i.e.*, E_{sup}) (Table S5) for all the matrices tested in this work (Table 1). Fig. 2 shows the values of I_{rel} (*i.e.*, relative signal

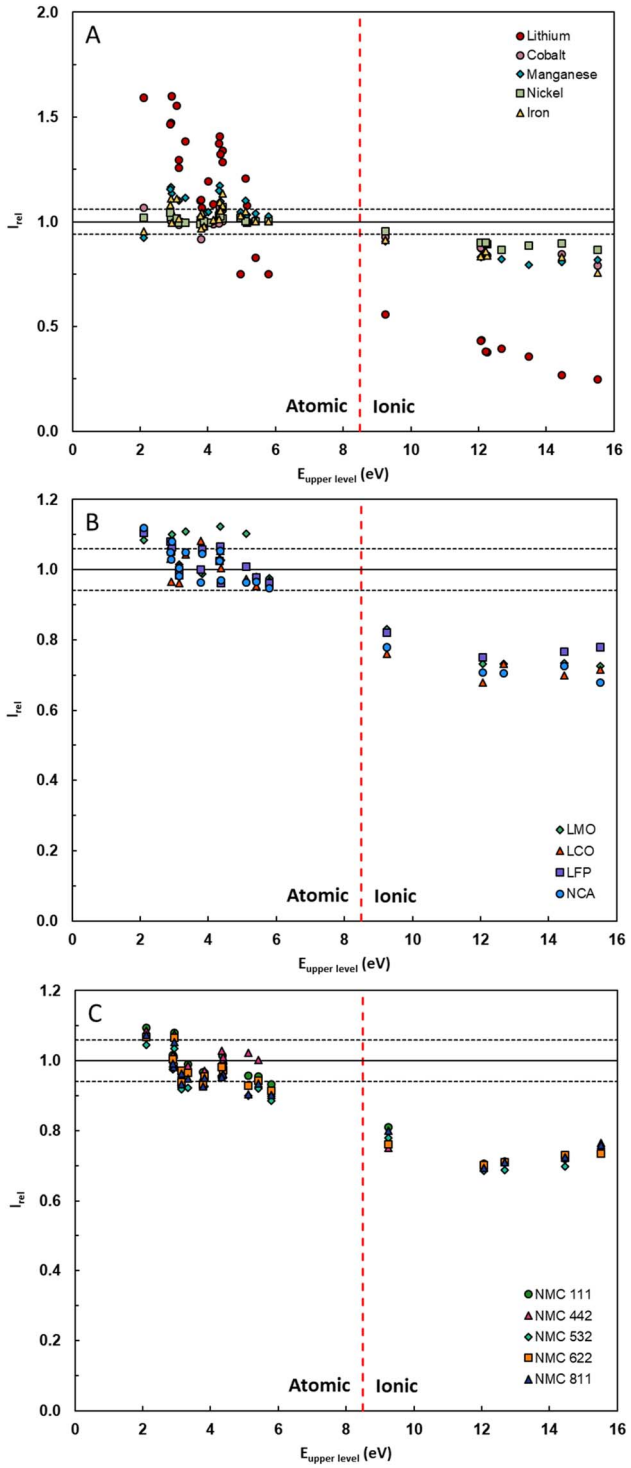

Fig. 2 Influence of the $E_{upper\ level}$ on the I_{rel} operating the solutions related to raw materials (A), binary (B) and ternary cathodes (C) regarding the reference solution (5% w w^{-1} HNO_3). Q_l 500 μL min^{-1}; Q_g 0.9 L min^{-1}; TExposure 1000 ms.

intensity), defined as the ratio between the net emission signal of an emission line obtained in a given matrix and that obtained when working with the reference one (*i.e.*, 5% w w^{-1} nitric acid), in relation to the $E_{upper\ level}$ of each emission line. The signal repeatability calculated was ~3% RSD (5 replicates), so it can be considered that I_{rel} values below 0.94 or higher than 1.06 (*i.e.* exceeding an uncertainty range of ± 6%) denote matrix effects.

In general, all ionic lines evaluated showed negative matrix effects, irrespective of the matrix considered, with particularly pronounced effects registered for the Li matrix. As regards the matrices related with the raw materials (Fig. 2A), the magnitude of the matrix effects increased with the $E_{upper\ level}$. In this case, I_{rel} values of approximately 0.94 (0.55 in the case of the Li matrix) were obtained for the least energetic ionic emission lines ($E_{upper\ level}$ = 9.2 eV) whereas I_{rel} values as low as 0.75, approximately (up to 0.25 for the Li matrix), were registered for the emission lines with higher $E_{upper\ level}$. Conversely, for the binary and ternary cathodes (Fig. 2B and C), I_{rel} values range between 0.7 and 0.8 for all the emission lines evaluated regardless of the matrix.

No significant changes in the atomic emission signal were observed for the matrices evaluated, apart from the Fe, Li and Mn matrices in the case of raw materials, and in certain atomic emission lines in the presence of cathode matrices. In general, positive matrix effects were registered for Fe and Mn with I_{rel} values about 1.15. In contrast, a more complex behaviour was observed for Li since matrix effects depended on the wavelength characteristics with I_{rel} values decreasing as $E_{upper\ level}$ increased (Fig. 2A). Indeed, a cross-over point between positive and negative matrix effects was observed. For atomic emission lines with $E_{upper\ level} < 4.5$ eV, positive matrix effects with I_{rel} values up to 1.55 were registered while for the most energetic ones ($E_{upper\ level} \geq 5$ eV) negative matrix effects were obtained (I_{rel} values up to 0.7). These results contrast to those reported by Hallwirth *et al.*,[27] who did not observe a correlation between the wavelength characteristics of the emission lines and the magnitude of matrix effects caused by Li. However, the trends exhibited in this work are consistent with those reported in previous studies operating saline solutions in MICAP OES and other high-power (N_2)-MIP cavities.[34,37] It is well-known that the introduction of easily ionizable elements into the plasma affects the ion–atom equilibrium due to the increase of the electron number density modifying the different excitation and ionization mechanisms that takes place into the plasma.[26,34,36,37] In the case of the transition metal elements (Co, Fe, Mn and Ni), they exhibit higher ionisation potentials (IP: Co 7.88 eV; Fe 7.90 eV; Mn 7.43 eV; and Ni 7.64 eV) than that of Li (IP: Li 5.3 eV) and, hence, changes in the electron number density are less significant due to the limited ionization degree.[38] Additionally, it should be considered that concentration levels for these species were approximately 10-fold lower (*i.e.* between 0.03 and 0.06 mol L^{-1}) than those of Li (0.3 mol L^{-1}) due to the composition of the materials and the higher dilution factor employed for the cathodes (*i.e.*, 1 : 100 and 1 : 200 dilution factors for raw materials and cathodes, respectively). Regarding the binary and ternary cathode matrices (Fig. 2B and C), it is interesting to highlight that atomic emission lines for some elements, such as Ca I 422.673 nm, Cu I 327.396 nm, Fe I 371.993 nm, Mg I 285.213 nm, Mg I 518.360 nm, and Na I 589.592 nm showed slight matrix effects with I_{rel} values about 1.09 and 1.12.

Therefore, as can be deduced from the previous data, the matrix effects and their magnitude depend on the composition of the matrix, that is, the type of material to be analysed. In the case of the raw materials, whenever there is Li, Mn and Fe in the matrix in high concentration levels (*i.e.*, LiOH, Li_2CO_3, $MnSO_4$ and $FePO_4$ materials), the signal of the ionic emission lines decreases, while for the atomic ones, in general, there is no matrix effect, with the exception of the Li matrix one. In the cathodes, independently of the sample composition, the ionic emission lines are affected along with the following atomic lines: Na I 589.592 nm, Ca I 422.673 nm, Fe I 371.993 nm, Cu I 327.396 nm, Mg I 285.213 nm, and Mg I 518.360 nm. Thus, special attention must be paid to the preparation of the calibration standards needed for the analysis of impurities and major elements in the different samples.

3.3 Calibration strategies

According to the Chinese standard protocols,[5–16] the impurities of interest in both raw materials and cathodes consist of the following elements: Al, B, Ca, Cd, Co, Cr, Cu, Fe, Mg, Mn, Na, Ni, Pb, Zn. For these elements, the most sensitive emission lines in MICAP OES are mainly atomic, except for Ca, Fe and Mn whose most sensitive emission line is ionic. Consequently, when analysing impurities in Li_2CO_3, LiOH, $MnSO_4$ and $FePO_4$ raw materials, matrix-matched calibration standards are the optimal strategy to mitigate matrix effects. Conversely, calibration standards prepared in 5% w w^{-1} nitric acid can be employed in the analysis of the $CoSO_4$ and $NiSO_4$ materials, although special attention must be paid to the Ca, Fe and Mn ionic lines. As regards cathode analysis, the most sensitive emission lines for Ca, Cu, Fe, Mn and Na (*i.e.*, Ca II 396.847 nm, Cu I 327.396 nm, Fe II 259.940 nm, Mn II 257.610 nm and Na I 589.592 nm), were interfered irrespective of the solution considered. Therefore, in order to analyse all the impurities simultaneously, matrix-matched calibration standards are recommended. However, if there is no interest in analysing the above-mentioned elements, calibration standards prepared in 5% w w^{-1} nitric acid may be employed.

As specified in the Chinese regulations, quality control also requires verifying the stoichiometry and the content of the major elements (Co, Li, Mn, and Ni) in the cathodes to ensure the performance of LiBs. However, given their elevated concentrations in the cathode materials, their analysis is troublesome since the linearity of the most sensitive emission lines is often limited by self-absorption and may even exceed the detector capabilities. It is therefore necessary to apply high dilution factors and, in some cases, to select less sensitive emission lines, to ensure an accurate quantification. In this case, an optimal dilution factor for cathodes was evaluated to ensure a minimum sample dilution to minimise errors. The minimum dilution factors employed ranged from 1 : 850 for NMC111, NMC442, NMC532, NMC622 and NMC 811 to 1 : 800 for the LFP cathode. However, these dilutions are not suitable for the simultaneous analysis of impurities and major elements in these samples, thus two different analyses should be performed instead.

Alternatively, to address the aforementioned issue and carry out the simultaneous analysis of both major elements and impurities in cathodes, the feasibility of reducing the time exposure, and, when necessary, employing less sensitive emission lines was evaluated. This approach aimed to allow sample analysis in a single run without compromising accuracy and improving sample throughput. To this end, the most sensitive emission lines were selected for impurities, whereas two different emission lines were considered for major elements (*i.e.*, the most sensitive line and another with lower sensitivity for some elements such as Co I 345.350 nm, Fe I 371.993 nm, Mn I 322.809 nm, Ni I 300.249 nm). Additionally, two different time exposures within the same run – 1000 ms for impurities and 40 ms for major elements – were selected. This approach was used to ensure that the sensitivity was high enough for the analysis of impurities and that the major elements were within the dynamic linear range (DLR). In this case, the use of matrix-matched calibration standards was mandatory for all the cathodes. Under these experimental conditions, both impurities and major elements could be analysed satisfactorily. Nonetheless, it is important to highlight that with this strategy the relative standard deviation (RSD) of the results was higher compared to the previous one. At lower time exposures, the DLR increased between 3 and 10-fold for all the major elements (*e.g.*, from 0.3–500 mg kg^{-1} to 0.7–3500 mg kg^{-1} for Co, 0.13–250 mg kg^{-1} to 0.7–2500 mg kg^{-1} for Fe or 0.05–150 mg kg^{-1} to 0.5–500 mg kg^{-1} for Li), but at the same time the RSD obtained increased by a factor of 9 (*i.e.*, from 0.1–1.1% to 3–9%). This fact can be attributed to the lower sensitivity of some of the emission lines selected and the lower period of time that the detector is recording the emission signal. Based on these findings, the selected operating conditions used to validate the method proposed consisted of a 1000 ms time exposure, a Q_g of 0.9 L min^{-1} and a Q_l of 500 μL min^{-1}. Matrix-matched calibration standards were used for trace elements, while calibration standards prepared in 5% w w^{-1} nitric acid were used for the analysis of major elements.

Table 2 Method limits of detection (mLODs) expressed as mg kg^{-1} of dry weight ($n = 3$) in MICAP OES for the different raw materials analysed. Q_g 0.9 L min^{-1}, Q_l 0.5 mL min^{-1}, TExposure: 1000 ms

Element	$CoSO_4$	$NiSO_4$	$MnSO_4$	$FePO_4$	Li_2CO_3	LiOH
Al I 396.152	1.0	1.0	0.6	0.6	1.0	1.0
B I 249.772	2	2	0.7	1.0	2	2
Ca II 396.847	0.04	0.04	0.3	0.14	0.09	0.09
Cd I 228.802	2	2	3	0.4	6	6
Co I 345.350	—	3	3	3	6	6
Cr I 428.973	1.3	1.3	0.6	0.9	1.0	1.0
Cu I 327.396	0.7	0.7	0.6	2	1.4	1.4
Fe II 259.940	2	2	5	—	2	2
Mg I 279.553	0.16	0.16	0.5	0.06	0.13	0.13
Mn II 257.610	1.0	1.0	—	0.4	2	2
Na I 589.592	0.4	0.4	4	0.3	0.4	0.4
Ni I 345.847	4	—	3	3	9	9
Pb I 405.781	4	4	20[a]	6	6	6
Zn I 213.857	7	7	5	6	3	3

[a] mLOD value calculated for the emission line Pb I 368.346 nm.

Table 3 Method limits of detection (mLODs) expressed as mg kg^{-1} of dry weight ($n = 3$) in MICAP OES for the different cathodes analysed. Q_g 0.9 L min^{-1}, Q_l 0.5 mL min^{-1}, TExposure: 1000 ms

Element	LCO	LFP	LMO	NCA	NMC111	NMC442	NMC532	NMC622	NMC811
Al I 396.152	9	4	13	5	20	7	13	5	13
Ca II 396.847	3	0.9	12	1.1	9	30	0.3	4	1.1
Cd I 228.802	30	3	30	40	6	30	30	30	20
Cr I 428.973	6	5	50	7	20	7	12	4	7
Cu I 327.396	9	13	13	6	13	2	4	2	13
Fe II 259.940	13	—	30	20	9	7	30	30	30
Mg I 279.553	0.2	3	5	0.7	2	0.9	3	1.3	5
Na I 589.592	2	2	5	7	7	0.7	13	0.7	5
Pb I 405.781	90	40	30[a]	100	12	30	30	50	30
Zn I 213.857	40	40	20	70	8	40	60	50	20

[a] mLOD value calculated for the emission line Pb I 368.346 nm.

3.4 Method validation

To evaluate the feasibility of MICAP OES for the quality control of raw materials and cathodes from LiBs, a certified reference material (*i.e.*, NMC111 BAM S014) and a wide range of raw materials (*e.g.*, Li_2CO_3, LiOH, $CoSO_4$, $MnSO_4$, $NiSO_4$ and $FePO_4$) and lithium-based cathodes (*e.g.*, LFP, LCO, LMO, NCA, and five NMCs with different stoichiometries) were employed to cover the diversity of materials currently found and used in the LiBs industry.

3.4.1 Limits of detection. The method limits of detection (mLODs) were calculated from the calibration curve for each sample (*i.e.*, matrix matched calibration standards and 1000 ms time exposure) according to the IUPAC guidelines and considering the dilution factors applied to each one.[39] The LOD values obtained, expressed as mg kg^{-1} of dry weight ($n = 3$), for the elements of interest according to the Chinese standard protocols for the raw materials and cathodes, are gathered in Tables 2 and 3, respectively. These mLOD data are equivalent to those afforded by ICP OES for both raw materials (0.02 μg L^{-1} for Ca and 0.27 μg L^{-1} for Na in a Li_2CO_3 raw material)[21] and cathodes analysis (between 0.02 and 8.7 mg kg^{-1} sample dry weight for Ca and Na, respectively, for a LFP cathode[40] and between 0.06 and 1.03 mg kg^{-1} for Cd and Na, respectively, for a NMC cathode[3]).[17–19]

In general, the mLOD values for cathodes were higher than those obtained for the raw materials. This may be related to the purity grade of the reagents employed to prepare the matrix-matched calibration standards and to the different dilution factors applied for each type of sample. It is interesting to note that the mLODs for Co, Fe, Li, Mn and Ni in these materials are not relevant as they were present in high concentrations. According to the Chinese standard protocols (Table S6), the mLOD values obtained for the raw materials allow the determination of almost all the impurities regulated in the different materials, with the exception of Pb and Zn in $CoSO_4$, $NiSO_4$ and Li_2CO_3, as well as, Cd in $NiSO_4$, Pb in $MnSO_4$, Al, Mn and Ni in Li_2CO_3, and Cu in LiOH. However, in the case of cathodes (Table S7), it is possible to analyse all the impurities regulated by means of MICAP OES as the mLODs values afforded are below the legal thresholds established. These differences between both types of samples arise from the impurity limits imposed on the raw materials, which are more restrictive (*i.e.*, in general one order of magnitude lower) than those applied to cathodes.

3.4.2 Trueness. The trueness, accuracy and precision, of the method was evaluated through the direct analysis of a certified reference material (NMC111 BAM S014) analysed in triplicate ($n = 3$) and recovery tests due to the unavailability of reference materials for the Li-based cathodes analysed and the raw materials. To this end, the raw materials and cathodes samples were fortified with the most relevant impurity elements according to the Chinese standards protocols, at 0.5 mg kg^{-1} of Al, B, Ca, Cd, Co, Cr, Cu, Fe, Mg, Mn, Na, Ni, Pb, Zn.

As can be observed in Table S8, the experimental values obtained for the major elements and impurities agreed with the certified ones and there was no significant difference for a p-value 0.05, with the exception of Cr. For this element, the certified value was below the mLODs, so it was not possible to determine its concentration. Regarding the recovery tests, according to the European conformity guidelines on the performance of analytical methods,[41] the trueness of a recovery test is considered successful if the deviation of the experimentally determined analyte concentration values and the spiked ones does not exceed the limit ± 10%. Fig. 3 shows the recovery values obtained for the Li_2CO_3 raw material and the NMC442 cathode as a representative of the results obtained. The remaining data are gathered in Fig. S4. In general, for raw materials, all the recovery values obtained were quantitative (range between 90 and 110%) except for Pb for the $MnSO_4$. As has already been mentioned, when operating matrices with high Mn levels, the most sensitive Pb wavelength (*i.e.*, Pb I 405.781 nm) is interfered and a less sensitive wavelength should be used instead (Pb I 368.346 nm). However, because Pb spiking levels were closed to the LoDs afforded by the latter line (0.2 mg kg^{-1}), accuracy and precision were significantly decreased. In the case of cathodes, recoveries for the different elements evaluated were quantitative independently of the composition. Furthermore, data acquired using MICAP OES were compared against ICP OES (a reference technique for LIBs characterization). No significant differences (±10%) were observed between them, as anticipated. Therefore, all these data demonstrated that MICAP OES is a suitable technique for the quality control of

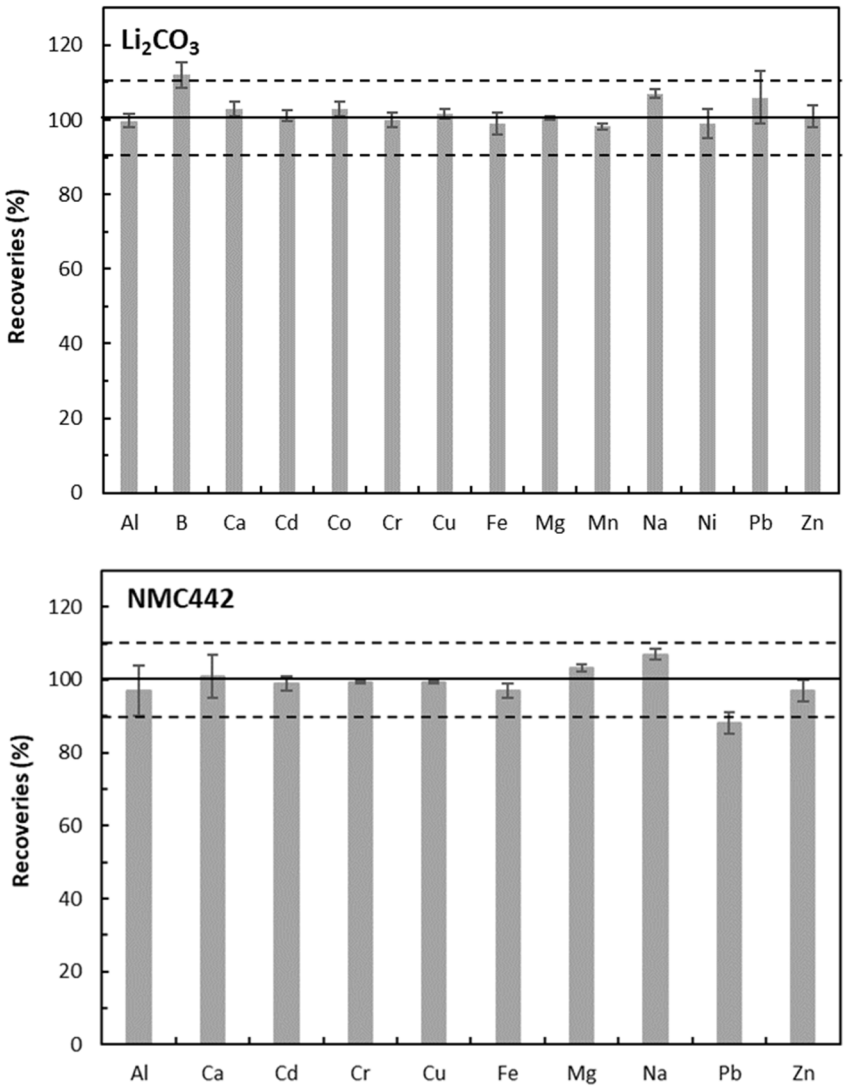

Fig. 3 Recoveries expressed as % (mean ± SD, $n = 3$) obtained for the Li_2CO_3 raw material and NMC442 cathode analysed by MICAP OES. Q_g 0.9 L min^{-1}, Q_l 0.5 mL min^{-1}, TExposure: 1000 ms.

Table 4 Impurity content in mg kg^{-1} (mean ± SD, $n = 3$) in the different raw material samples analysed by MICAP OES. Q_g 0.9 L min^{-1}, Q_l 0.5 mL min^{-1}, TExposure: 1000 ms

Element	$CoSO_4$	$NiSO_4$	$MnSO_4$	$FePO_4$	Li_2CO_3	LiOH
Al I 396.152	<1	<1	<0.6	<0.6	20.2 ± 0.4	<1
B I 249.772	<2	<2	<0.7	10.1 ± 0.2	60.1 ± 1.2[a]	40.5 ± 0.4
Ca II 396.847	10.1 ± 0.3	10.2 ± 0.2	<0.3	7.23 ± 0.14	40 ± 2	8.6 ± 0.4
Cd I 228.802	<2	<2	<3	<0.4	<6	<6
Co I 345.350	—	500 ± 10	<3	<3	<6	<6
Cr I 428.973	<1.3	<1.3	<0.6	4.3 ± 0.1	<1	<1
Cu I 327.396	<LoD	<0.7	<0.6	30 ± 2	24.2 ± 0.5[a]	18 ± 2[a]
Fe II 259.940	<2	<LoD	<5	—	<2	<2
Mg I 279.553	3.93 ± 0.06	170 ± 3	<0.5	2.9 ± 0.1	8.1 ± 0.2	3.1 ± 0.4
Mn II 257.610	<1	<1	—	500 ± 10	16.5 ± 0.3[a]	14.6 ± 0.4[a]
Na I 589.592	2.21 ± 0.12	190 ± 4	<4	60.5 ± 1.2	100 ± 2	30.2 ± 0.4
Ni I 345.847	<4	—	<3	<3	<9	<9
Pb I 405.781	<4	<4	<20	<6	<6	<6
Zn I 213.857	<7	300 ± 6[a]	<5	50 ± 2	<3	<3

[a] These values are outside the limits established in the Chinese standard protocols.[5–10]

Table 5 Major (in %) and impurity content (in mg kg^{-1}) (mean ± SD, $n = 3$) in the different cathodes samples analysed by MICAP OES. Q_g 0.9 L min^{-1}, Q_l 0.5 mL min^{-1}, TExposure: 1000 ms

Element	LCO	LFP	LMO	NCA	NMC111	NMC442	NMC532	NMC622	NMC811
Al I 396.152	—	—	—	0.9 ± 0.2	—	—	—	—	—
Co I 240.725	50 ± 4[a]	—	—	8.53 ± 0.07	20.3 ± 1.0	12.21 ± 0.12	11.96 ± 0.12	11.75 ± 0.09	6.92 ± 0.03
Fe I 371.993	—	36.77 ± 0.14	—	—	—	—	—	—	—
Li I 610.364	7.5 ± 0.3	3.97 ± 0.02	7.85 ± 0.08[a]	6.79 ± 0.17	6.9 ± 0.3	8.27 ± 0.09	7.48 ± 0.08	7.91 ± 0.04	7.69 ± 0.06
Mn I 280.106	—	—	59.4 ± 0.7	—	16.0 ± 1.0	21.9 ± 0.2	16.11 ± 0.15	10.71 ± 0.09	3.01 ± 0.02
Ni I 300.249	—	—	—	47.3 ± 0.5	20.2 ± 1.0	24.6 ± 0.3	28.9 ± 0.3	35.4 ± 0.3	47.8 ± 0.3
Al I 396.152	1835 ± 9	45.8 ± 0.3	69 ± 4	—	<20	65.6 ± 0.9	52 ± 2	1170 ± 50	941 ± 4
Ca II 396.847	26 ± 3	51 ± 6	276.9 ± 0.8	86 ± 8	49.4 ± 0.9	17 ± 3	235 ± 3	91 ± 3	21 ± 4
Cd I 228.802	16.4 ± 1.0	<3	<30	<40	<6	<30	<30	<30	<20
Cr I 428.973	<6	21 ± 2	<50	<7	<20	<7	<12	<4	<7
Cu I 327.396	<9	40 ± 4	17.1 ± 1.9	15 ± 2	48.1 ± 0.6	<2	25.0 ± 1.0	18.6 ± 1.5	15 ± 2
Fe II 259.940	34 ± 3	—	37 ± 4	11.6 ± 0.7	<9	<7	58.4 ± 0.9	51.3 ± 0.8	55 ± 3
Mg I 279.553	1651 ± 12	25.4 ± 0.3	51.5 ± 1.1	178 ± 2	21.2 ± 0.8	40.4 ± 0.9	161.9 ± 1.0	113.08 ± 0.04	35.3 ± 0.3
Na I 589.592	98 ± 4	45.0 ± 1.3	214 ± 14	15.7 ± 1.3	89.1 ± 1.1	96 ± 6	55 ± 2	99.8 ± 1.9	40 ± 2
Pb I 405.781	<90	140 ± 10	<30	<100	<12	<30	<30	<50	<30
Zn I 213.857	<40	95 ± 7	14.5 ± 1.3	<70	<8	215.0 ± 0.2	332.56 ± 0.08[a]	317 ± 3[a]	408 ± 15

[a] These values are outside the limits established in the Chinese standard protocols.[11–16]

LiBs related materials. Regarding the precision of the method (*i.e.*, relative standard deviation), it was within the 0.1–4% range for all the elements evaluated regardless of the sample considered. The method reproducibility was evaluated by analyzing three independent replicates of each sample on five different days, and it was lower than 7% for all the samples tested.

3.4.3 Sample analysis. According to Chinese standard protocols, for raw materials, the control of impurities is important to ensure the final quality of the batteries, while for cathodes, both impurities and the stoichiometry of each of the elements that compose them can affect the quality and determine the performance of the batteries. Therefore, all LiBs related samples employed through this work were analysed according to these guidelines. All samples were analysed by means of MICAP OES after digestion. Tables 4 and 5 show the impurity concentration levels found for the raw materials, and both the major elements and impurities determined for cathodes, respectively. For raw materials, the content of impurities lied between the limits set by the different Chinese standard regulations for half of the samples analysed, while the content of B, Cu and Mn for Li_2CO_3, Cu and Mn for LiOH, and Zn for $NiSO_4$ were higher than the less restrictive limits defined according to the characteristics of each material and its use (Table S6). It is interesting to note that, all the values obtained for $MnSO_4$ were below the mLODs. Nonetheless, these values would be below the most restrictive limits defined for this raw material according to the Chinese standard protocols, with the exception of Pb. In this case, the mLOD obtained for Pb (*i.e.*, 20 mg kg^{-1}) with the emission line employed (Pb I 368.346 nm), was higher than the limit set in the regulation (10 or 15 mg kg^{-1}). Consequently, an alternative technique such as ICP-MS would be required to accurately determine Pb in this raw material, due to its superior sensitivity and detections limits.

In the case of the cathodes, it can be observed that for 3 of the NMC cathodes (*i.e.*, NMC532, NMC622 and NMC 811) the Zn concentration level found lies outside of the limit defined (300 mg kg^{-1}) (Table S7). Regarding the stoichiometry of the main elements, the LCO and LMO samples did not fulfil the requisites of the regulations (Table S9) since the Co concentration in LCO was lower than the established content (*i.e.*, 57-60%), and Li in the LMO cathode was higher than the allowed concentration (*i.e.*, 4.2 ± 0.4 mg kg^{-1}).

4. Conclusions

In this study, a novel analytical methodology is proposed for the quality control of LiBs industry materials (*i.e.*, raw materials and cathodes) by means of MICAP OES in accordance with the available regulations. Both impurities and major elements can be simultaneously determined in a single run by the appropriate selection of operating conditions and the calibration strategies (*i.e.*, matrix-matched calibration standards and lower time exposures). Special care is required for Pb determination in Mn-containing matrices due to the spectral interference of Mn on the most sensitive Pb wavelength. Although the method remains susceptible to matrix effects caused by sample concomitants (mainly Li), changes in both atomic and ionic emission can be satisfactorily corrected using matrix-matched calibration standards. Moreover, the analyte figures of merit shown by MICAP OES are comparable to those afforded by ICP OES, making it a suitable technique for quality control applications within LiBs related materials. Finally, it is important to highlight that, according to the results discussed, the proposed methodology could also be extended to the quality assessment of materials recovered from LiB-based black mass, supporting its relevance in both manufacturing and recycling contexts.

Conflicts of interest

The authors declare that they have no known competing financial interests or personal relationships that could have appeared to influence the work reported in this paper.

Data availability

Supplementary information: the data supporting this article have been included as part of the SI. See DOI: https://doi.org/10.1039/D5JA00183H.

Acknowledgements

The authors would like to thank the University of Alicante for the financial support of this work (VIGROB-050). J. Pérez would like to thank the University of Alicante for the given fellowship (UAFPU22-22). The authors would also like to thank Dr Carlos Abad Andrade and the Inorganic Reference Materials unit at the Federal Institute for Materials Research and Testing (BAM) for providing us with several of the materials used in this study.

References

1 S. Nowak and M. Winter, *J. Anal. At. Spectrom.*, 2017, **32**, 1833, DOI: 10.1039/C7JA00073A.
2 A. M. Theodore, *J. Chem. Res.*, 2023, **47**, DOI: 10.1177/17475198231183349.
3 J. He, X. Li, F. Wang, M. Jing, and J. Cui, Thermo Fisher application note, 73872, (Last access March 2025), https://assets.thermofisher.com/TFS-Assets/CMD/Application-Notes/an-73872-icp-oes-elements-lithium-batteries-an73872-en.pdf.
4 H. H. Heimes, A. Kampker, A. vom Hemdt, K. D. Kreisköther, S. Michaelis, and E. Rahimzei, *Manufacturing of Lithium-Ion Battery Cell Components*, RWTH AACHEN University, 2019, ISBN: 978-3-947920-07-5.
5 *Non-Ferrous Metal Industry Standard of The People's Republic of China, Battery Grade Lithium Carbonate*, YS/T 582-2023, 2023.
6 *National Standard of The People's Republic of China, Battery Grade Lithium Hydroxide Monohydrate*, GB/T 26008-2020, 2020.
7 *Chemical Industry Standard of The People's Republic of China, Cobalt Sulfate for Battery Materials*, HG/T 5918-2021, 2021.
8 *Industry Standard of The People's Republic of China, Manganese Sulfate for Battery Materials*, HG/T 4823-2015, 2015.
9 *Chemical Industry Standard of The People's Republic of China, Nickel Sulfate for Battery Materials*, HG/T 5919-2021, 2021.
10 *Industry Standard of The People's Republic of China, Iron Phosphate for Batteries*, HG/T 4701-2021, 2021.
11 *Non-Ferrous Metal Industry Standard of The People's Republic of China, Lithium Nickel Cobalt Manganese Oxide*, YS/T 798-2012, 2012.
12 *National Standard of The People's Republic of China, Lithium Cobalt Oxide*, GB/T 20252-2014, 2014.
13 *Non-Ferrous Industry Standard of The People's Republic of China, Lithium Iron Phosphate*, YS/T 1027-2015, 2015.
14 *National Standard of The People's Republic of China, Lithium Nickel Manganese Oxide*, GB/T 37202-2018, 2018.
15 *Non-Ferrous Metal Industry Standard of The People's Republic of China, Lithium Manganese Oxide*, YS/T 677-2016, 2016.
16 *Non-Ferrous Metal Industry Standard of The People's Republic of China, Lithium Nickel Cobalt Aluminum Oxide*, YS/T 1125-2016, 2016.
17 Y. Qi and N. Drvodelic, Agilent application note, Last access March 2025, https://www.agilent.com/cs/library/applications/an-lithium-carbonate-5800-icp-oes-5994-6112en-agilent.pdf.
18 Spectro analytical instruments, Spectro application note, (Last access March 2025), https://www.spectro.com/landingpages/icp-oes-arcos-application-analysis-of-lithium-composite-oxide-cathode-materials.
19 F. Wenkun, and N. Yingping, Agilent application note, (Last access March 2025), https://www.agilent.com/cs/library/applications/application_lithium_impurities_icp-oes_5110_5991-9506en-us-agilent.pdf.
20 A. Suárez, A. Jara, R. Castillo and K. Gallardo, *ACS Omega*, 2024, **9**, 20129–20134, DOI: 10.1021/acsomega.4c00085.
21 S. Sengupta and D. Kutscher, Thermo Fisher application note, 001178, (Last access March 2025), https://assets.thermofisher.com/TFS-Assets/CMD/Application-Notes/an-001168-tea-icp-oes-icap-pro-xp-lithium-carbonate-an001168-na-en.pdf.
22 L. Fu, H. Xie, J. Huang, X. Chen and L. Chen, *Spectrochim. Acta, Part B*, 2021, **18**, 106217, DOI: 10.1016/j.sab.2021.106217.
23 B. M. Fontoura, F. C. Jofré, T. Williams, M. Savio, G. L. Donati and J. A. Nóbrega, *J. Anal. At. Spectrom.*, 2022, **37**, 966–984, DOI: 10.1039/D1JA00375E.
24 A. Muller, D. Pozebon and V. L. Dressler, *J. Anal. At. Spectrom.*, 2020, **35**, 2113–2131, DOI: 10.1039/D0JA00272K.
25 C. B. Williams, R. S. Amais, B. M. Fontoura, B. T. Jones, J. A. Nóbrega and G. L. Donati, *Trends Anal. Chem.*, 2019, **116**, 151–157, DOI: 10.1016/j.trac.2019.05.007.
26 R. Serrano, G. Grindlay, L. Gras and J. Mora, *J. Anal. At. Spectrom.*, 2019, **34**, 1611–1617, DOI: 10.1039/C9JA00148D.
27 F. Hallwirth, M. Wolfgang and H. Wiltsche, *J. Anal. At. Spectrom.*, 2023, **38**, 1682–1690, DOI: 10.1039/D3JA00061C.
28 O. V. Pelipasov and E. Polyakova, *J. Anal. At. Spectrom.*, 2020, **35**, 1389–1394, DOI: 10.1039/D0JA00065E.
29 K. A. M. L. Cruz, G. L. Donati, F. R. P. Rocha and M. C. Hespanhol, *Anal. Methods*, 2023, **15**, 3675–3682, DOI: 10.1039/D3AY01035J.
30 A. J. Schwartz, Y. Cheung, J. Jevtic, V. Pikelja, A. Menon, S. T. Ray and G. M. Hietje, *J. Anal. At. Spectrom.*, 2016, **31**, 440–449, DOI: 10.1039/C5JA00418G.
31 K. M. Thaler, A. J. Schwartz, C. Haisch, R. Niessner and G. M. Hieftje, *Talanta*, 2018, **180**, 25–31, DOI: 10.1016/j.talanta.2017.12.021.
32 M. Kuonen, G. Niu, B. Hattendorf and D. Günther, *J. Anal. At. Spectrom.*, 2023, **38**, 758–765, DOI: 10.1039/D2JA00369D.
33 A. Winckelmann, J. Roik, S. Recknagel, C. Abad and Z. You, *J. Anal. At. Spectrom.*, 2023, **38**, 1253–1260, DOI: 10.1039/D3JA00088E.
34 R. Serrano, G. Grindlay, L. Gras and J. Mora, *Talanta*, 2024, **271**, 125666, DOI: 10.1016/j.talanta.2024.125666.
35 J. Pérez-Vázquez, A. García-Juan, R. Serrano, G. Grindlay and L. Gras, *Microchem. J.*, 2025, **213**, 113655, DOI: 10.1016/j.microc.2025.113655.

36 Z. Zhang and K. Wagatsuma, *Spectrochim. Acta, Part B*, 2002, **57**, 1247–1257, DOI: **10.1016/S0584-8547(02)00049-6**.
37 R. Serrano, E. Anticó, G. Grindlay, L. Gras and C. Fontás, *Talanta*, 2022, **240**, 123166, DOI: **10.1016/j.talanta.2021.123166**.
38 R. S. Houk, *Anal. Chem.*, 1986, **58**, 97–105, DOI: **10.1021/ac00292a003**.
39 J. Inczédy, T. Lengyel, A. M. Ure, A. Gelencsér, and A. Hulanicki, *IUPAC Analytical Chemistry Division, Compendium of Analytical Nomenclature*, 3rd edn, Blackwell, Oxford, 1998.
40 J. He, X. Li, F. Wang, M. Jing, and J. Cui, Thermo Fisher application note, 000245, (Last access March 2025), **https://assets.thermofisher.com/TFS-Assets/CMD/Application-Notes/an-000245-tea-icp-oes-lithium-iron-phosphate-impurities-an000245-na-en.pdf**.
41 2002/657/EC, *Consolidated text: European Commission Decision of 12 August 2002 Implementing Council Directive 96/23/EC Concerning the Performance of Analytical Methods and the Interpretation of Results*.